

## Mimicking PAMAM Dendrimers with Amphoteric, Hybrid Triazine Dendrimers: A Comparison of Dispersity and Stability

Sanjiv Lalwani,<sup>\*,†</sup> Abdellatif Chouai, Lisa M. Perez, Vanessa Santiago, Sunil Shaunak,<sup>‡</sup> and Eric E. Simanek<sup>\*,†</sup>

<sup>†</sup>Department of Chemistry, Texas A&M University, College Station, Texas 77843, and <sup>‡</sup>Faculty of Medicine, Imperial College London, Hammersmith Hospital, Ducane Road, London, W12 0NN, U.K.

Received June 2, 2009; Revised Manuscript Received July 17, 2009

**ABSTRACT:** Two strategies are applied to mimic the amphoteric nature of the surfaces of half-generation PAMAM dendrimers yet retain the very narrow dispersity inherent of triazine dendrimers. Both strategies start with a monodisperse, single-chemical entity, generation two triazine dendrimer presenting 12 surface amines that is available at the kilogram scale. The first method relies on reaction with methyl bromoacetate. Complete conversion of the surface primary amines to tertiary amines occurs to provide 24 surface esters. Extended reaction times lead to quarternization of the amines while other unidentified species are also present. The resulting polyester can be quantitatively hydrolyzed using 4 M aqueous HCl to yield a dendrimer with 12 tertiary amines and 24 carboxylic acids about a hydrophobic triazine core. The second method utilizes Michael additions of methyl acrylate to yield 24 surface esters. This reaction proceeds more rapidly and more cleanly than the former strategy. Hydrolysis of this material proceeds quantitatively using 4 M aqueous HCl to yield the desired dendrimer. In both cases, MALDI–TOF mass spectrometry provides compelling evidence of reaction progress. Electrophoretic analysis confirms the amphoteric nature of these materials with the former targets having a pI value in the  $1.8 < \text{pI} < 3.4$  range, and the latter having a pI value in the  $4.7 < \text{pI} < 5.9$ . These ranges bookend the pH range within which PAMAM dendrimers become zwitterionic,  $3.4 < \text{pI} < 4.7$ . The strategy of using monodisperse amine-terminated dendrimer constructs as core offers significant advantage over PAMAM homopolymers including dispersity, ease of characterization and batch-to-batch reproducibility. These triazine dendrimers could ultimately be adopted into materials with applications wherein the demands of purity have hitherto remained unsatisfied.

### Introduction

The impact of polyamidoamine (PAMAM) dendrimers across diverse fields including applications in therapeutics,<sup>1,2</sup> diagnostics,<sup>3</sup> sensing,<sup>4</sup> material science,<sup>5</sup> and catalysis<sup>6</sup> since Tomalia's first report<sup>7</sup> cannot be understated. Indeed, PAMAM or Starburst dendrimers are the most extensively studied family of these materials.<sup>8</sup> PAMAM dendrimers are commercially available with amine terminal groups referred to as full-generation dendrimers, or with carboxylate terminal groups referred to as half-generation dendrimers. Full-generation dendrimers can have a cationic or a neutral surface depending on the pH. Half-generation dendrimers have an amphoteric (and under certain pH conditions, zwitterionic) surface. With these materials going into preclinical trials<sup>9</sup> precise knowledge of the structural complexity of these dendrimeric nanodevices becomes increasingly important.<sup>10</sup> Significant effort has been invested in characterizing these materials using a combination of corroborative methods.<sup>11</sup> In general, PAMAM materials exist as highly complex mixtures: the two-step iterative polyamidoamine chemistry utilized in PAMAM dendrimer synthesis introduces the possibility of nonideal dendrimer growth through a variety of factors that affect the monodispersity of the growing polymer.<sup>7</sup> Retro-Michael reactions account for another source of structural heterogeneity.

As an alternative to PAMAM dendrimers, our efforts have been toward providing single-entity dendrimers that can be synthesized reproducibly and with high purity: we use

2,4,6-trichloro-1,3,5-triazine (cyanuric chloride), a low-cost and readily available reagent. Using this chemistry, kilogram-scale synthesis of a generation two triazine dendrimer<sup>12</sup> has been reported that used only a single chromatographic step and which provided materials judged conservatively as being approximately 93% pure based on reversed-phase HPLC analysis of the BOC-protected intermediate. Higher purities can be achieved if intermediates are subjected to more rigorous purification than the precipitation strategy utilized in the scale-up procedure. Recently, this material was used in the synthesis of anionic triazine dendrimers derived from the succinylation of generation two and generation three amine-terminated triazine dendrimers.<sup>13</sup> Analysis of these materials using capillary electrophoresis (CE) in comparison to the commercially available PAMAM analogues showed a significant difference in molecular heterogeneity: PAMAM dendrimers were highly disperse mixtures whereas triazine dendrimers approached single-chemical-entity materials.

Full-generation (amine terminated) and half-generation (carboxylate terminated) PAMAM dendrimers have shown markedly different behavior in biological applications: in a report by Malik et al., amine-terminated PAMAM dendrimers displayed generation-dependent hemolysis and changes in red cell morphology whereas anionic dendrimers were neither hemolytic, nor cytotoxic;<sup>14</sup> El-Sayed et al. reported increased paracellular permeability within a "size window" of generation 2.5 and 3.5 PAMAM carboxylate terminated dendrimers;<sup>15</sup> an investigation on the effect of PAMAM dendrimers on planar phosphatidyl choline membranes by Shcharbin et al.<sup>16</sup> showed that cationic PAMAM generation 5 dendrimer disrupted the membranes

\*To whom correspondence should be addressed. E-mail: simanek@mail.chem.tamu.edu.

whereas carboxylate-terminated PAMAM generation 4.5 dendrimer did not. From these demonstrated examples, and many more, it is evident that the surface chemistry and topology of dendrimers is a critical parameter in their applications-based utility.

In this paper, we report the synthesis and characterization of amphoteric triazine dendrimers obtained using two strategies. The first scheme involves reacting methyl bromoacetate with generation two amine-terminated triazine dendrimer, followed by exhaustive hydrolysis of the ester groups. Two hydrolysis conditions are tested: use of 4 M HCl and 5 M NaOH, both at room temperature. The rates of ester hydrolysis and purity of final products in the tested conditions are compared. Overall, the first scheme yields a triazine dendrimer bearing 24 acetate groups. Similarly, in the second scheme, generation two amine-terminated triazine dendrimer is reacted with methyl acrylate via Michael addition to result in a material with 24 surface ester groups. Subsequent hydrolysis of this material was affected in 4 M aqueous HCl and 5 M NaOH. Overall, the second scheme resulted in a triazine dendrimer displaying 24 propionate groups. From our work on the succinylation of triazine dendrimers<sup>13</sup> it was observed that progress of the succinylation reaction can be meticulously followed using MALDI-TOF MS and CE: mass spectrometry identifies the species present in the mixture at the end of the reaction and CE provides quantitative information on purity. As such, the synthesis of the ester-bearing intermediates and the carboxylate-bearing final products was closely monitored using MALDI-TOF MS. Purity and molecular heterogeneity assessments were obtained using CE and were compared with commercially available PAMAM analogues. PAMAM dendrimers with the diaminobutane (DAB) core were selected for comparison instead of ethylenediamine (EDA) core analogues because of their inherent interest to the group, their broader spectrum of use, and lower dispersity as indicated by slab gel electrophoresis in the available product literature.

## Experimental Section

**Materials.** All reagents and solvents needed in the synthesis and the analysis of triazine dendrimers were purchased from Aldrich Chemical Co. (Milwaukee, WI) and were used as received. Uncoated fused silica capillaries were purchased from Polymicro Technologies, LLC, (Phoenix, AZ). Commercial half-generation, diaminobutane-core PAMAM carboxylate dendrimers were also purchased from Aldrich Chemical Co. The second generation triazine dendrimer used in this work was synthesized in our laboratory as previously reported.<sup>12</sup>

**Synthesis of 1e.** A solution of the generation two amine-terminated triazine dendrimer was prepared by dissolving 50.0 mg (0.0169 mmol) of the solids into 2.0 mL of the appropriate solvent (methanol or tetrahydrofuran). To this was added methyl bromoacetate (37.2 mg, 22.4  $\mu$ L, 0.244 mmol) corresponding to 1.2 molar equiv per  $\text{NH}_2$ . The reaction mixture was allowed to stir at room temperature for 2 h. Formation of a white precipitate was observed (presumably the hydrobromide salt of the partially substituted dendrimer). Then, 68.7  $\mu$ L of a separately prepared methanolic solution of potassium hydroxide (prepared by dissolving 206 mg of solid potassium hydroxide in 1.0 L of methanol under rigorous stirring) was added to the dendrimer-containing reaction mixture. The mixture was stirred at room temperature and sample was taken for analysis by MALDI-TOF MS after 14 h of reaction time. Further additions of 1.2 molar equiv of methyl bromoacetate per  $\text{NH}_2$  were required, each one accompanied by the addition of 68.7  $\mu$ L of the methanolic potassium hydroxide solution. Progress of the reaction was monitored using MALDI-TOF MS. A total of 8.4 molar equiv of methyl bromoacetate per  $\text{NH}_2$  had been added when signals corresponding to 25- and 26-ester-bearing

dendrimers were observed along with the desired 24-ester-bearing species, as well as signals corresponding to incompletely substituted dendrimers.

<sup>1</sup>H NMR ( $\text{CDCl}_3$ ):  $\delta$  5.35–4.70 (br m), 4.70–3.30 (br m), 3.30–2.89 (br m), 2.67–1.00 (br m). <sup>13</sup>C NMR ( $\text{CDCl}_3$ ):  $\delta$  175.9–163.6, 125.6, 61.7–59.7, 55.4–54.2, 52.7–51.2, 47.3–42.6, 41.5–38.5, 30.3, 29.7, 28.3–24.1.

**Synthesis of 1a.** An aliquot of the reaction mixture corresponding to 10.0 mg of dendrimer 1e was taken, and the solvent was removed under reduced pressure. The glassy material that remained was dissolved in 400  $\mu$ L of 4 M HCl and allowed to react at room temperature. Progress of the hydrolysis reaction was monitored using MALDI-TOF MS. A 200  $\mu$ L aliquot of the solution was then transferred into a preconditioned Centricon centrifugal filter device (Amicon Bioseparations) having a regenerated cellulose membrane with a 3,000 molecular weight cutoff. The retained solution was collected and used as is for further analysis.

<sup>1</sup>H NMR ( $\text{D}_2\text{O}$ ):  $\delta$  4.00–2.70 (br m), 2.60–2.15 (br s), 2.04–0.41 (br m). <sup>13</sup>C NMR ( $\text{D}_2\text{O}$ ):  $\delta$  179.8–178.3, 167.1–163.7, 59.5–57.9, 54.4–51.3, 45.5–41.4, 26.4–23.6.

**Synthesis of 2e.** A solution of the generation two amine-terminated triazine dendrimer was prepared by dissolving 300 mg (0.101 mmol) of the solids into 5.0 mL of methanol under constant stirring. To this solution, 252 mg (263  $\mu$ L, 2.92 mmol) of methyl acrylate was added slowly, corresponding to 2 molar equiv per  $\text{NH}_2$  and a corresponding 20% mol/mol excess per addition. The reaction mixture was allowed to stir at room temperature. Samples were taken over time and analyzed by MALDI-TOF MS. Reaction was deemed complete after 3 days of reaction time.

<sup>1</sup>H NMR ( $\text{CDCl}_3$ ):  $\delta$  4.00–3.00 (br m), 2.90–2.00 (br m), 1.97–1.13 (br m). <sup>13</sup>C NMR ( $\text{CDCl}_3$ ):  $\delta$  173.4–172.6, 166.5–164.3, 125.5, 51.9–50.9, 49.4–48.5, 45.8–44.7, 44.6–43.5, 43.4–42.6, 39.2–36.4, 32.7–31.8, 30.2, 28.6–27.1, 26.4–24.6.

**Synthesis of 2a.** An aliquot of the reaction mixture corresponding to 10.0 mg of dendrimer 2e was taken, and the solvent was removed under reduced pressure. The glassy material that remained was dissolved in 400  $\mu$ L of 4 M HCl and allowed to react at room temperature. Progress of the hydrolysis reaction was monitored using MALDI-TOF MS which showed complete hydrolysis of the esters within 2 days. A 200  $\mu$ L aliquot of the solution was then transferred into a preconditioned Centricon centrifugal filter device (Amicon Bioseparations) having a regenerated cellulose membrane with a 3000 molecular weight cutoff. The retained solution was collected and used for further analysis as is.

<sup>1</sup>H NMR ( $\text{D}_2\text{O}$ ):  $\delta$  4.19–2.77 (br m), 2.76–2.22 (br s), 2.20–0.41 (br m). <sup>13</sup>C NMR ( $\text{D}_2\text{O}$ ):  $\delta$  177.9–175.5, 167.0–163.5, 51.6–47.9, 46.0–41.1, 30.3–28.0, 26.2–23.6, 23.3, –20.6.

**Capillary Electrophoresis.** A P/ACE MDQ capillary electrophoresis system with a photodiode array detector (Beckman-Coulter, Fullerton, CA) was used to obtain all of the CE separations. Uncoated fused silica capillaries were treated according to the coating procedure described by Kaneta et al.<sup>17</sup> using poly(vinylpyrrolidone) as a semipermanent coating. Capillaries used had an internal diameter of 50  $\mu$ m and typical lengths as follows: total length of the capillary,  $L_t$ , 30.6 cm; length of the capillary from injection point to the detection window,  $L_d$ , 20.7 cm. Lengths  $L_t$  and  $L_d$  varied from cartridge-to-cartridge by  $\pm 0.5$  cm.

The different background electrolytes (BGEs) used were made by first preparing a solution of the buffering species of the desired concentration, followed by titration to the desired pH using the titrant in the pure form (as solid or liquid). Further details on the selection of BGE components and preparation are provided as part of the Supporting Information. Solutions of 0.2–0.5% dimethyl sulfoxide (DMSO) in water were used as the neutral marker. All purity and dispersity analysis were performed using conventional CE protocols (i.e., capillary rinse;

pressure injection of sample; optional pressure injection of neutral marker; electrophoresis) whereas determination of pH ranges which bracket the respective isoelectric points of the dendrimers were determined by pressure-mediated capillary electrophoretic (PreMCE) separations.<sup>18</sup>

**MS Characterization.** MALDI–TOF mass spectra were performed on a ABI Voyager-DE STR mass spectrometer operating in reflected mode using 2,4,6-trihydroxyacetophenone (THAP) as matrix. When needed, MS data was reprocessed using Origin 8 and Microsoft Excel software packages.

**NMR Spectroscopy.** <sup>1</sup>H and <sup>13</sup>C NMR spectroscopy was performed using either Mercury 300 or an Inova 300 instrument. Since broad and overlapping signals are observed, chemical shifts are reported as ranges.

**Computation.** Computational results were obtained using the software package Materials Studio (MS) 4.4 (Accelrys, Inc.). The dendrimers were built in the fully extended conformation using the dendrimer builder tools in MS. The conformational space of each dendrimer was sampled via 300 Simulated Annealing (SA) cycles over a period of 840 ps using the Forcite Plus program and the polymer consistent force-field (pcff) as implemented in MS 4.4. The SA runs utilized constant volume and temperature (*NVT*) molecular dynamics (MD) over a temperature range of 300–1000 K using the Nosé thermostat,  $\Delta T = 50$  K, untruncated atom-based electrostatic and van der Waals interactions, and a time step of 1 fs. The dendrimer was minimized after each annealing cycle, resulting in 300 minimized structures per dendrimer. Electrostatic potential maps were generated at the AM1 level of theory using the vasp program as implemented in MS for the lowest energy conformation of each dendrimer obtained from the SA simulations.

## Results and Discussion

**Nomenclature.** Scheme 1 shows the synthesis of the target dendrimers from a previously reported, generation two dendrimer with 12 amine groups. Reaction with methyl bromoacetate yields **1e**, a generation 2.5 (adopting the PAMAM nomenclature) hybrid dendrimer wherein the “e” reflects the ester periphery.<sup>12</sup> Hydrolysis yields the polyacid, **1a**. Similarly, reaction with methyl acrylate yields **2e** that is subsequently hydrolyzed to polyacid **2a**.

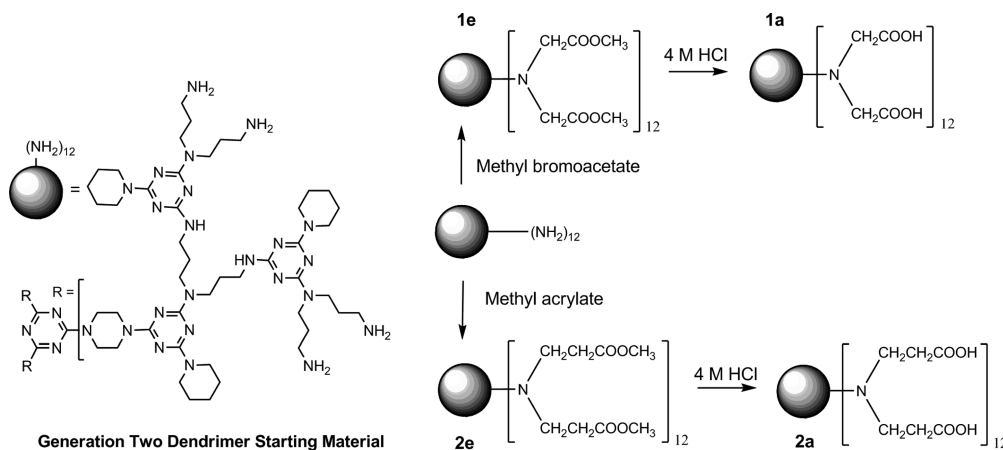
**Synthesis of 1e and 1a.** Reaction of the generation two amine-terminated triazine dendrimer with methyl bromoacetate was attempted in two solvents, methanol and tetrahydrofuran. Aliquots were removed to monitor the progress of the reaction by MALDI–TOF MS. Figure 1 shows the traces obtained for the reaction in methanol. The starting material shows a single line at  $m/z$  2954. Panels A and B capture the reaction at 3 h and 1 day. The characteristic

separation of 72 mass units corresponding to the primary ladder of peaks represents additional “CH<sub>2</sub>COOCH<sub>3</sub>” groups. The numbers above the peaks correspond to the number of additions. The suggestion of greater complexity in panel B and clear presence in panel C results from (i) the detection of both proton and potassium adducts and (ii) undesired ester hydrolysis. Potassium adducts are prominent due to the use of KOH as a base in the reaction. Finally, panel D provides clear warning against the overinterpretation of mass data. Here, as a function of ionization conditions, it is possible to obtain spectra that show intermediates wherein only an even number of substitutions have occurred including prominent lines at 18, 20, 22, and the desired 24 substitutions. Optimizing ionization conditions allows for the expected spectra. Curiously, we are unable to suppress the even products in favor of the odd as a function of ionization conditions or matrix. The Supporting Information details some of these matrix effects, and as a result, we decided to use 2,4,6-trihydroxyacetophenone (THAP) throughout this study. The spectrum shown in panel E reveals a limitation to this chemistry. At increasing reaction times, an additional species that we attribute to a cyclization product (lactam) becomes increasingly abundant.

As eluded to, closer inspection of the data reveals an even richer description of the chemistries (Figure 2). Again, numbers above the peaks correspond to the number of methyl acetate units on the molecule. Four signals are observed for each substitution: peaks corresponding to the proton adduct (labeled as **a**) and potassium adduct (labeled as **c**) in addition to peaks labeled as **b** and **d** at  $m/z$  values of 14-less than signals labeled as **a** and **c** respectively, corresponding to the loss of a methyl group (hydrolysis). These lines result from the use of a methanolic solution of potassium hydroxide to scavenge the hydrobromic acid produced in the reaction. Another potential side reaction, the substitution of the bromide functionality in the unreacted methyl bromoacetate with a hydroxyl group also occurs. Although this would not affect the number of signals observed in the mass spectrum, the occurrence of such side reaction is evident from the amount of excess reagent required to drive the reaction to completion.

Further, the nature of the chemistry employed does not provide sufficient control over the formation of tertiary amine versus quaternary ammonium bearing products as evident from mass spectra for the reaction in tetrahydrofuran obtained after 5 days of reaction time at room temperature (Figure 3, bottom trace). While complete substitution has not yet been achieved, as revealed by lines corresponding

Scheme 1. Synthesis of the Hybrid Dendrimers





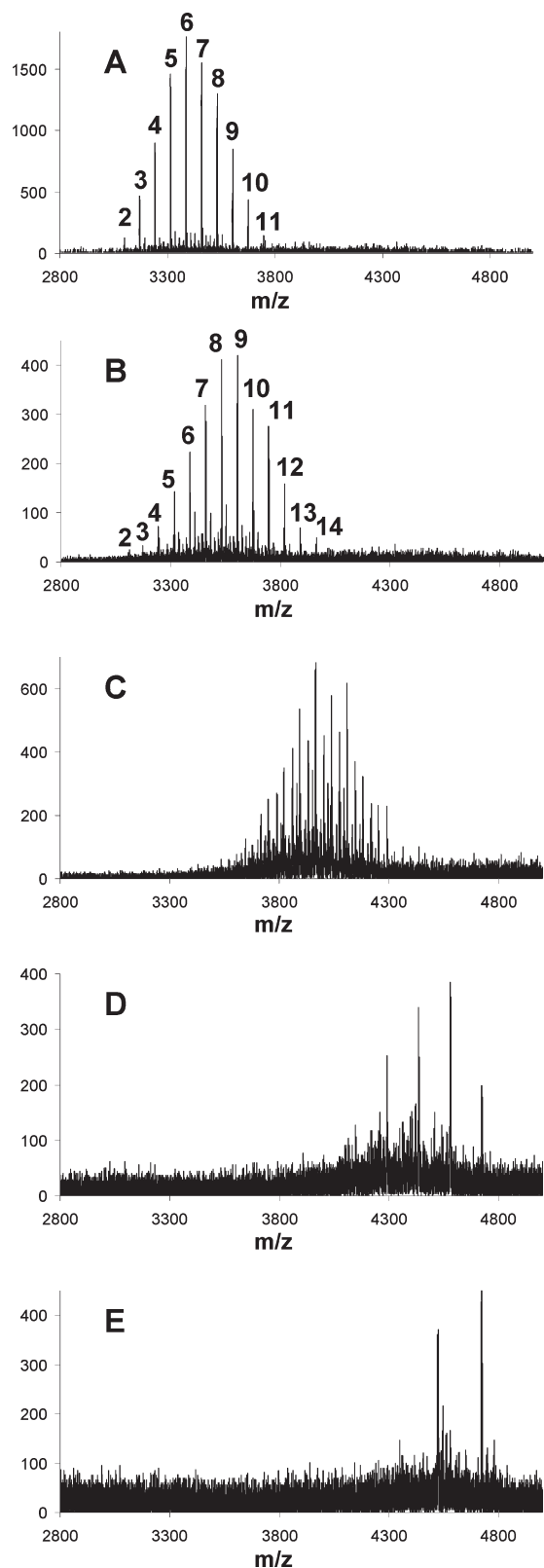


**Figure 1.** MALDI-TOF MS traces for aliquots taken from the reaction mixture for the synthesis of **1e** using methanol as the solvent. Number above the peaks represents the number of methyl acetate substitutions on the generation two triazine dendrimer. The corresponding reaction times are as follows: (A) 3 h; (B) 1 day; (C) 5 days; (D) 6 days; (E) 11 days.

to 22 and 23 methyl acetate substitutions in addition to the desired product, we also observe signals corresponding to products with 1 and 2 quaternary ammonium groups. Just as

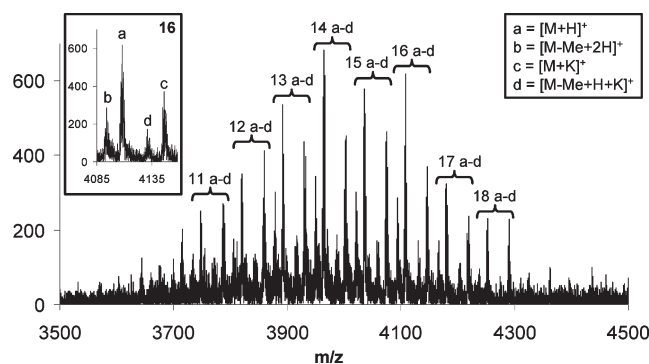


**Figure 2.** MALDI-TOF MS trace for an aliquot of the reaction mixture for the synthesis of **1e**. The number above the set of peaks represents the number of methyl acetate substitutions on the generation two triazine dendrimer. The legend for the corresponding peaks a-d is indicated as an inset in the spectrum.

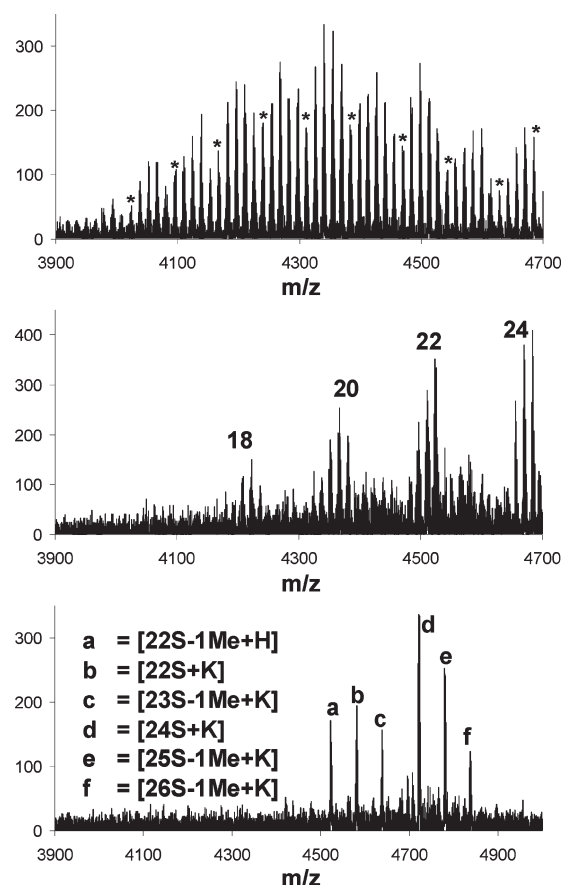


**Figure 3.** MALDI-TOF MS traces for aliquots taken from the reaction mixture for the synthesis of **1e** using tetrahydrofuran as the solvent. Spectrum obtained after 1 day of reaction time (top trace) shows 15–24 substitutions on the generation two triazine dendrimer (marked with “\*”) and signals decreasing by steps of  $m/z = 14$  corresponding to increasing ester hydrolysis. Spectrum obtained after 4 days (middle trace) shows prevalent signals for species with even number of substitutions whereas signals for species with an odd number of substitutions appear to be disfavored. Spectrum obtained after 5 days (bottom trace) shows products ranging from 22 to 26 substitutions (abbreviated as 22S to 26S), derivatives due to ester hydrolysis and potassium adducts thereof.

in the previous case, complicated spectra due to undesired ester hydrolysis (Figure 3, top trace) and varying ionization tendencies are also observed in these samples, as evident from the change in the relative intensities of signals corresponding to species with odd- and even-numbered

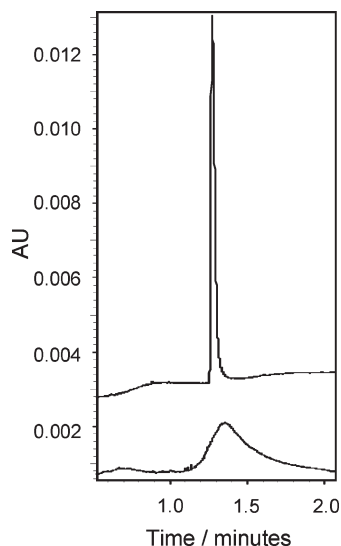


**Figure 4.** CE traces for **1e** (bottom trace) and **2e** (top trace) obtained using a pH 3.4 100 mM formate/lithium buffer.

additions of methyl bromoacetate (top and middle traces in Figure 3).

A sample from the tetrahydrofuran-containing reaction mixture was analyzed by capillary electrophoresis, CE, using a pH 3.4, 100 mM formate/lithium background electrolyte (BGE). Under these conditions, **1e** and other dendrimeric products of the reaction are expected to migrate as cations. Electrophoresis was therefore performed using a positive-to-negative polarity setup, where the positively charged electrode is placed near the point of injection and the negatively charged electrode is placed near the outlet end of the capillary. The bottom trace in Figure 4 shows the electropherogram. The observed peak width for **1e** indicates a more diverse composition than **2e**. This is in agreement with results of MALDI-TOF MS analysis, which indicates the presence of both incompletely substituted dendrimer products and those containing quaternary ammonium groups. Further, CE provides hints toward the structural diversity of this mixture. Due to the use of a pH 3.4 BGE for analysis using CE, resolution between species having a different number of ester groups is not expected, since the cationic character of the molecule does not change (number of charge-bearing amines remains constant). This is also true when quaternary ammonium groups are formed, as even the secondary amines are expected to be fully protonated at a pH of 3.4. However, the cationic character of the dendrimer can decrease by two paths: (i) ester hydrolysis and (ii) amide bond formation with either the free methyl bromoacetate or intramolecular cyclization. In both cases, cations having a migration velocity slightly slower than the desired product **1e** will be generated. Incomplete resolution of these dendrimers will result in a greater peak width. We believe both of the mentioned processes contribute to the observed dispersity.

Products from the interrupted synthesis of **1e** were subjected to hydrolysis in 4 M HCl solution at room temperature. Aliquots were taken after 1, 4, 10, and 22 days of reaction and analyzed by MALDI-TOF MS (Figure 5). After 10 days, significant incomplete hydrolysis of the esters was observed (data not shown) whereas by the 22nd day only the completely hydrolyzed and 1-ester-group-bearing species are observed. The pattern showing dendrimer species with three different degrees of substitution as seen in the initial sample was preserved throughout the course of the hydrolysis reaction. Intentional hydrolysis in 5 M NaOH

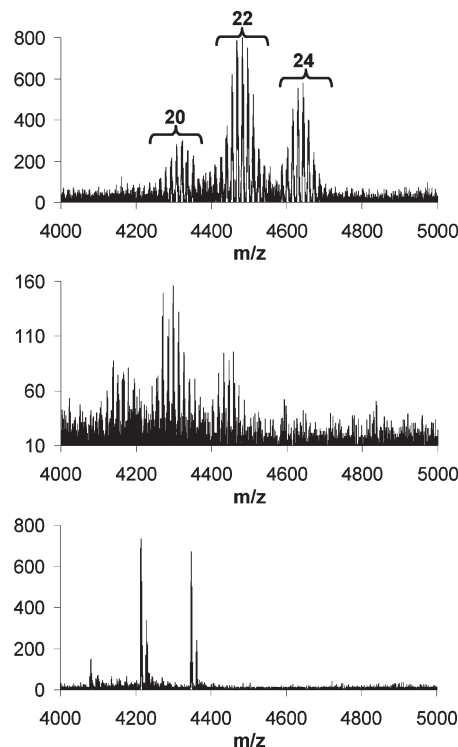


**Figure 5.** MALDI-TOF MS traces for aliquots of the reaction mixture wherein **1a** is produced from the hydrolysis of the esters of **1e** recorded after reaction times of 1 day (top trace), 4 days (middle trace) and 22 days (bottom trace). The spectra reveal different degrees of substitution: sets of signals corresponding to triazine dendrimers with 20, 22, and 24 substitutions are observed. Within each set, peaks separated by an  $m/z$  of 14 indicate an increasing number of ester groups still present.

proceeded much more rapidly: complete hydrolysis was observed in two days at room temperature as determined using MALDI-TOF MS (data shown as part of Figure 9). Overall, it appears unlikely that single-entity triazine dendrimers can be obtained using this chemistry. Nonetheless, as shown in the MS and CE analysis of the final products, the synthesized triazine dendrimers are still of significantly higher purity in comparison with the commercially available PAMAM analogues.

**Synthesis of **2e** and **2a**.** While reaction with methyl bromoacetate produces materials that resemble the structure of PAMAM dendrimers, using methyl acrylate exactly mirrors PAMAM chemistry. Indeed, the strategy proves remarkably clean and straightforward. Samples of the reaction between the triazine dendrimer and methyl acrylate were analyzed over a 3-day period using MALDI-TOF MS. Figure 6 shows the traces that were obtained. As a consequence of starting with a well-characterized amine-terminated dendrimer, the addition of each methyl acrylate unit onto the dendrimer can be observed (panel A recorded after 1 day of reaction time). Mass spectrum obtained after 3 days at room temperature is very simple and easy to interpret: one major signal corresponding to a dendrimer **2e** with 24 propionate esters and two minor signals corresponding to species with 22 and 23 substitutions (panel B).

This choice of chemistry offers several advantages. First, due to the nature of the Michael reaction, addition of base to the reaction is not required, and as such, hydrolysis of the ester groups is not observed. Also, a large excess of the active reagent (methyl acrylate) is not needed: the reaction proceeds close to completion with just 20% mol/mol excess reagent (per addition) within the 3-day reaction time at room temperature.

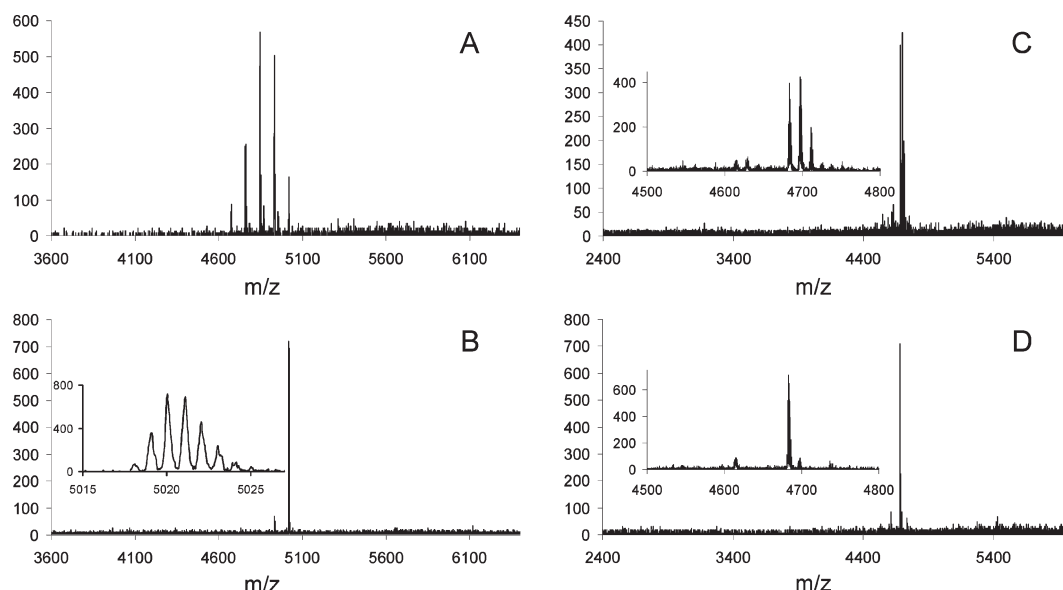


**Figure 6.** MALDI-TOF MS traces for aliquots of the reaction mixture for the synthesis of **2e** (panels A and B) and for the synthesis of **2a** (panels C and D). Peaks in panel A are separated by an  $m/z$  of 86 indicating an increasing number of methyl acrylate additions; panel B shows dendrimer with 23 and 24 additions. Inset in panel C shows peaks separated by an  $m/z$  of 14 indicating incomplete hydrolysis of the ester groups. Lastly, panel D shows two peaks separated by an  $m/z$  of 72, indicating products with 23 and 24 carboxylic acids.

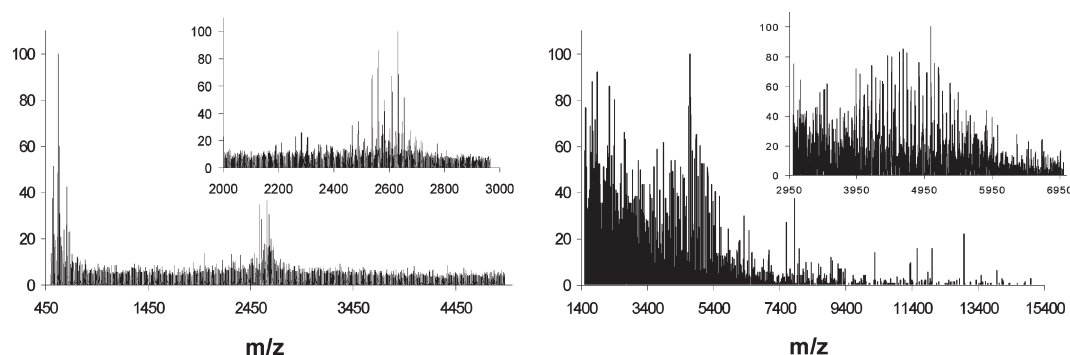


**Figure 7.** MALDI-TOF MS spectra of generation 1.5 (left panel) and generation 2.5 (right panel) PAMAM dendrimers bearing 16 and 32 carboxylic acid groups, respectively. The number of carboxylic acid groups is based on an ideal structure and signals with lower mass units observed may be due to dendrimers with structural defects.

A sample of the reaction mixture from the synthesis of **2e** was analyzed using CE. Identical conditions to those described earlier were used: a pH 3.4, 100 mM formate/lithium solution as BGE and a positive-to-negative polarity setup. Under the chosen conditions, the desired product **2e** and other products of the reaction are expected to migrate as cations. The bottom panel in Figure 4 shows the obtained electropherogram. The single and narrow peak observed, in comparison to the first derivative, **1e** (top panel), must be treated with tempered enthusiasm as there are limitations to this analysis: the method is unable to resolve species having a different number of ester groups unless accompanied by a different number of amines (as is the case with amide formation). Indeed, MALDI-TOF MS indicates the presence of dendrimers substituted 22 and 23 times. However, these derivatives are not resolved by our CE method.

Hydrolysis was affected by a strong acid instead of a strong base to limit retro-Michael reactions. Hydrolysis in 4 M HCl solution at room temperature was followed using MALDI-TOF MS and was found to proceed cleanly: the three-peak-pattern for dendrimers with different number of added methyl acrylates observed prior to hydrolysis was seen in both an intermediate sample (Figure 6, panel C) and the final sample upon complete hydrolysis (Figure 6, panel D).

The spectrum for the final sample showed a major signal corresponding to the dendrimer **2a** with 24 propanoic groups as well as the side products, dendrimers with 22 and 23 acids. These materials prove to be much cleaner than the corresponding PAMAM dendrimers available to us commercially (Figure 7) as observed using both MALDI-MS and capillary electrophoresis (Figure 8).

**Comparison of Dispersity.** The dispersity of the synthesized hybrid triazine dendrimers and the commercially available PAMAM analogues was compared by two means: MALDI-TOF MS and CE. Shown in Figure 7 are the MS traces obtained for generation 1.5 and generation 2.5 diamino-butane core-PAMAM dendrimers. On the basis of the ideal structure of the dendrimer, signals corresponding to  $m/z$  values of 2610 and 5588 are expected for the two materials. However, the obtained MS traces show a significantly greater number of signals in the 2200 to 2800 and the 3400 to 6500  $m/z$  ranges for the two dendrimer samples, respectively, indicating a complex mixture of dendrimer molecules having nonideal structures. The notion that PAMAM analogues of the hybrid triazine dendrimers reported in this work are highly complex mixtures is further corroborated by analysis using CE. Figure 8 shows the electropherograms obtained for the four dendrimers analyzed in this

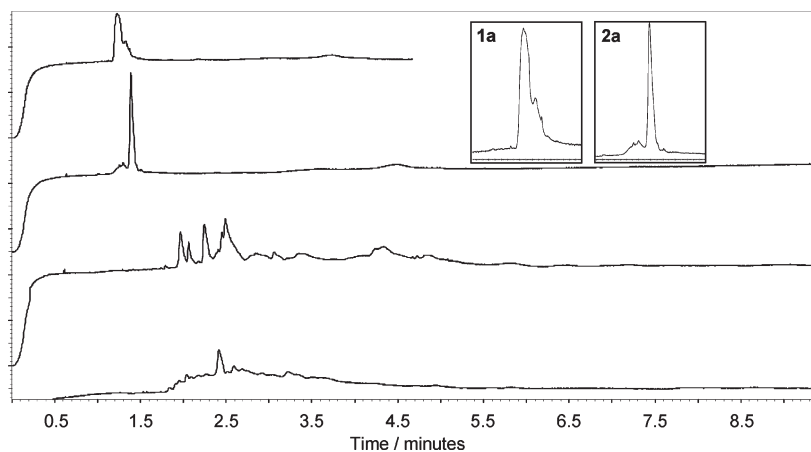


**Figure 8.** Electropherograms for the dendrimers included in this study obtained using a pH 6.9, 50 mM phosphate/lithium BGE in negative-to-positive polarity: **1a** (top trace), **2a** (second trace), PAMAM G1.5 (third trace), and PAMAM G2.5 (bottom trace).

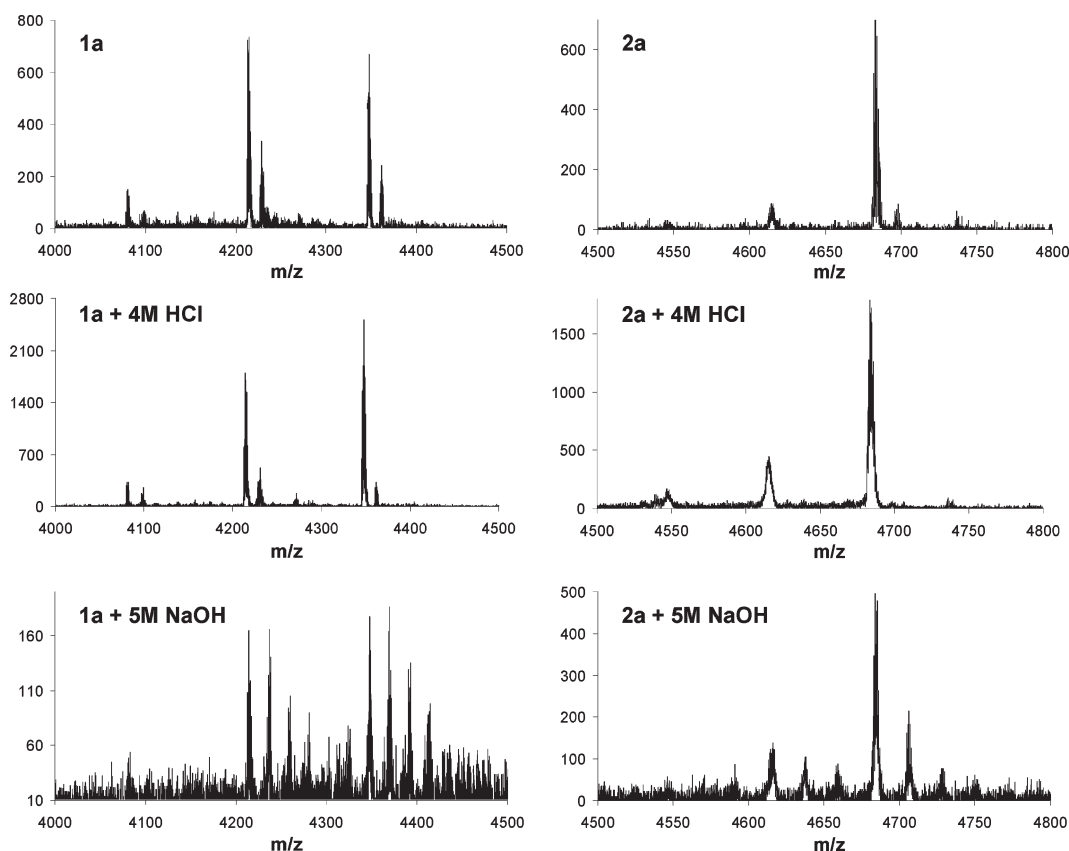


**Figure 9.** MALDI–TOF MS traces for **1a** (left) and **2a** (right) obtained to determine their stability under relatively harsh conditions: top traces were obtained from samples immediately after hydrolysis of the corresponding ester precursors; middle traces were obtained after storage in 4 M HCl and bottom traces were obtained after storage in 5 M NaOH (signals in the bottom traces separated by an  $m/z$  of 22 result from species with multiple sodium counterions).

work. Analysis was performed using a pH 6.9, 50 mM phosphate/lithium buffer using negative-to-positive polarity (negatively charged electrode is placed near the injection end of the capillary and positively charged electrode is placed near the outlet end). The choice of BGE was guided by our previous work on the development of a CE method for analysis of anionic dendrimers.<sup>13</sup> Unlike the CE analysis of **1e** and **2e** where a pH 3.4 BGE was used, here we expect to be able to resolve species based on differences in both the cationic and anionic characters is of the dendrimer.

The drastic difference in dispersity between triazine and PAMAM dendrimers is obvious: traces for **1a** and **2a** (top

and second from the top respectively) show a major component and some minor components whereas traces obtained for generation 1.5 and generation 2.5 PAMAM dendrimers (second from the bottom and bottom trace respectively) show a highly complex mixture of species where it becomes difficult to determine which of the observed signals represents the dendrimer having the ideal structure.

Furthermore, we were interested in quantifying the purity of the ideal dendrimer **2a** as this proved to be present as the least disperse mixture. Although the pH 6.9 phosphate/lithium buffer provided sufficient resolution, the fear of interference from the “system peak” (aka eigenpeak)

generated close to the dendrimer signals prevented reliable integration. On the basis of simulation experiments using the Peakmaster software package<sup>19</sup> an alternative BGE was determined: a 100 mM, pH 6.5 BisTris/acetate BGE did not generate system peaks with mobility values close to that of the analyte. Using this BGE, the resolution remained unchanged and the major signal in the trace for dendrimer **2a** was found to integrate to a corrected area of ~80% relative to the other observed signals (data not shown). Integration of signals was not relevant for the other derivatives due to the dispersity and/or low resolution, and thus further analysis on these samples was not performed.

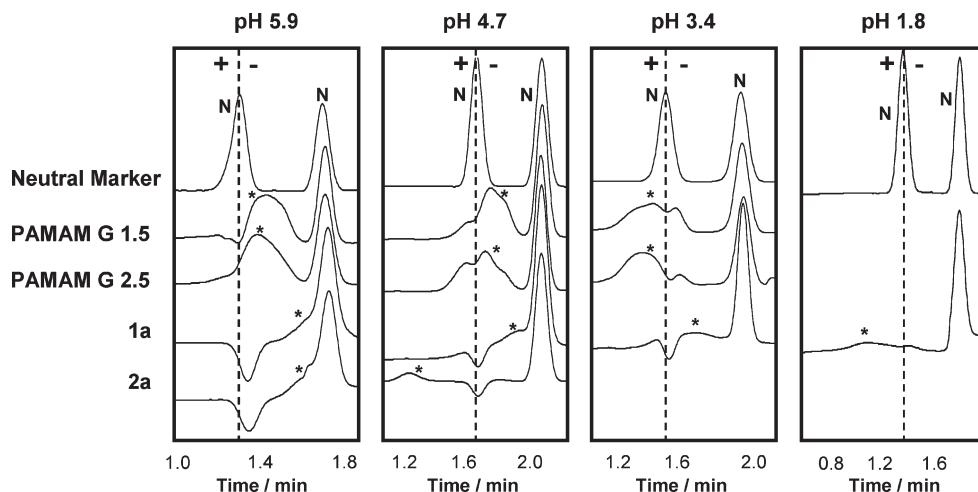
**Comparison of Stability.** Peterson et al. showed that PAMAM half-generation dendrimers are highly susceptible to degradation in the +50 °C to -15 °C temperature range.<sup>20</sup> Our objective was to determine the structural integrity of the synthesized hybrid dendrimers in two extremely harsh conditions: 4 M aqueous HCl solution and 5 M NaOH solution. Shown in Figure 9 are the MS traces obtained for the two samples. Each panel has been labeled to indicate the corresponding dendrimer and consists of three traces representing: initial sample (top), sample stored in 4 M HCl (middle trace) and sample stored in 5 M NaOH (bottom trace). It is evident from the preserved three-species-pattern, based on the number of substitutions on the triazine core, for the hybrid dendrimer **1a** that noticeable degradation has not occurred in either of the two conditions. In the case of the hybrid triazine dendrimer **2a**, species corresponding to less than 22 substitutions are not observed, and only a slight change in the relative intensities of signals is seen, regardless of whether the sample was stored for 21 days in 4 M HCl (middle trace) or for 3 days in 5 M NaOH (bottom trace), although the latter conditions lead to multiple sodiated species. The slight change in relative intensities may be due to the conditions favoring degradation via retro-Michael reactions or may simply be an artifact attributed to possible changes in the efficiency of ionization in MS.

**Comparison of pI Values.** To compare the isoelectric point (pI) values of **1a** and **2a** with their PAMAM analogues, the method of Glukhovskiy and Vigh<sup>21</sup> was adopted, where pressure-mediated CE (PreMCE) was used to determine the mobility of the dendrimers in BGEs having different pH values. Both the effective mobility of the analyte and the

mobility due to the electroosmotic flow can be calculated from the traces obtained using this method. However, since the objective was to compare the charge state of these dendrimers under different pH conditions, a simple determination of whether the analyte band was moving as an anion or as a cation suffices. The charge state on the dendrimer can be inferred from the direction in which it migrates with respect to a neutral marker as a result of the applied potential: under our chosen conditions, if the distance between the bands increases, it can be inferred that the analyte migrated as a cation. If the opposite is true, the analyte migrated as an anion. Additional details of the technique are provided in the Supporting Information.

Our previous work<sup>13</sup> established that half-generation PAMAM dendrimers migrate as anions at pH 6.9. Accordingly, we expect pI values for these dendrimers and their triazine analogues to be less than 6.9. The mobility of these dendrimers under varying conditions using BGEs with pH values of 1.8, 3.4, 4.7, and 5.9 were determined (details as to the formulation of the BGEs are given in the Supporting Information). Figure 10 shows the obtained PreMCE traces (only relevant portions shown), separated into panels corresponding to the BGE used. Each trace consists of two signals: the first trace in each panel shows two signals corresponding to two distinct neutral marker bands within the capillary whereas the first signal in succeeding traces corresponds to the dendrimer being analyzed and the second signal corresponds to the neutral marker acting as a mobility reference. A common artifact in all of the traces is a “system peak” (aka eigenpeak) which appears at the same location as a neutral marker. In the presence of a neutral marker, this artifact is not observed, however, in the absence of a neutral marker (as in the case of the dendrimer samples) this system peak appears as a dip overlapping with the signal corresponding to the dendrimer making it appear as if the analyte band was split with some of the components migrating as cations and others as anions.

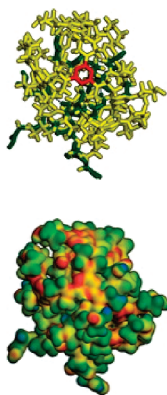
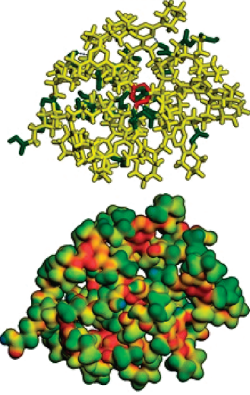
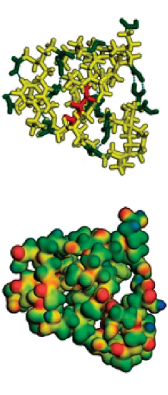
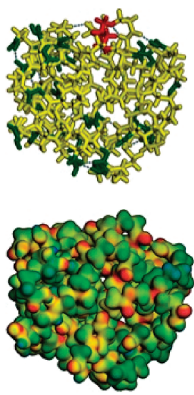
Traces that were obtained using a pH 5.9 BGE are shown in the first panel from the left. All of the dendrimers migrate as anions. When a pH 4.7 BGE is used (second panel from the left), triazine dendrimer **2a** migrates as a cation, whereas all other dendrimers continue to migrate as anions, indicating the pI for **2a** is in the 4.7 < pI < 5.9 range. Use of a pH



**Figure 10.** Traces obtained using pressure-mediated capillary electrophoresis for PAMAM and triazine dendrimers at different pH values: pH 5.9 (first panel), pH 4.7 (second panel), pH 3.4 (third panel) and pH 1.8 (fourth panel). Neutral marker signals are labeled as “N”; dendrimer signals are labeled with an asterisk. Dashed line from the centroid of the first neutral marker in the first trace of each panel serves as a guide: analytes that migrate to the left of the line migrate as cations, those migrating to the right migrate as anions. The dip observed in-line with the first neutral marker results from a comigrating system peak.



Table 1. Summary of Physical and Computational Data<sup>a</sup>

| Cmpd: <b>1a</b>   | <b>2a</b>   | <b>PAMAM 1.5</b>   | <b>PAMAM 2.5</b>  |
|---|---|--|---|
|  |  |  |  |
| 3° Amines: 12<br>Triazinyl: 30  | 3° Amines: 12<br>Triazinyl: 30  | 3° Amines: 14  | 3° Amines: 30   |
| COOH: 24  | 24  | 16   | 32  |
| 1.8 < pI < 3.4  | 4.7 < pI < 5.9  | 3.4 < pI < 4.7   | 3.4 < pI < 4.7  |
| Dia.: 1.8 nm  | 1.9 nm  | 1.5 nm   | 2.0 nm  |

<sup>a</sup> The cores of the dendrimers are shown in red and the terminal carboxylic acid groups shown in green. Stick representations show the lowest energy structure obtained from the SA calculations. AM1 electrostatic potential maps range from  $-0.2$  kcal/mol (red) to  $0.2$  kcal/mol (blue) mapped on the  $0.02 \text{ \AA}^{-3}$  electron density surface. The number of amine and carboxylate groups are based on idealized structures for the targets. Triazinyl amines are counted to include the exocyclic nitrogen and aromatic ring nitrogen as a single unit, a strategy that undercounts the nitrogen atoms by  $2\times$ , but may overcount proton-accepting sites by  $3\times$  if the triazine unit is only protonated once.

3.4 BGE (third panel) places the pI value for the PAMAM dendrimers in the  $3.4 < \text{pI} < 4.7$  since PAMAM dendrimers migrate as cations in this BGE. Triazine dendrimer **1a** migrates as an anion in BGEs with pH values above 3.4, and migrates as a cation in a pH 1.8 BGE (shown in the last panel) and so its pI value must fall within the  $1.8 < \text{pI} < 3.4$  range. Having such low pI values is an important property for these dendrimers as this results in a net-anionic charge on the respective dendrimers under neutral conditions, bestowing upon them high aqueous solubility, such as that observed for many proteins with pI values greater than or less than 7 (e.g., human albumin, a common protein in serum has a pI of 4.7<sup>22</sup>).

The difference in pI values between the different dendrimers can be explained based on the structure of the molecules. On the basis of the difference between the  $\text{pK}_a$  values for the carboxylic acids of glycine (2.36)<sup>23</sup> and  $\beta$ -alanine (3.53)<sup>23</sup> triazine dendrimer **1a** is expected to have the lowest pI value among all of the dendrimers tested. The two PAMAM dendrimers are expected to have similar pI values: in both cases the number of amines is equal to two less than the number of carboxylic acids and the  $\text{pK}_a$  values for both the carboxylic acids and amines are not expected to be significantly different. The triazine dendrimer **2a** however is expected to have a higher pI value than the PAMAM dendrimers due to the additional contribution to the basic (and cationic) character of the dendrimer coming from the protonation of the triazine ring nitrogens ( $\text{pK}_a$  for the ring nitrogens of melamine, a model compound, is 5.1<sup>24</sup>).

**Computation.** To complete this comparison of PAMAM and hybrid triazine dendrimers, computation analyses were performed. Table 1 summarizes the results of these studies as well as a summary of other physical characteristics. All four molecules are sufficiently small that the red core (triazine or diaminobutane) groups have access to the surface. The acid

groups on the periphery are shown in green and hydrogen-bonding interactions between these groups as well as with the backbone are observed. Both the gas-phase diameters of these species and the amount of free volume within the structure are visually similar. The calculated radii of gyration (reported as diameter) corroborate this expectation, although G1.5 PAMAM is a flattened structure that leads to a smaller number. This porosity is perhaps the only clue to the nonproteinaceous (that is, well-organized and tightly packed) nature of these macromolecules. Triazine groups of the hybrid dendrimers are readily evident in yellow/orange hues on the electrostatic potential maps. The high degree of similarity in these structures leads us to hypothesize that these hybrid dendrimers could serve as well-defined surrogates for low generation PAMAM materials. This similarity, however, must be taken with some caution, as it derives from gas-phase calculations. While valuable, these calculations invariably lead to densely packed structures that may not adequately communicate differences in solution. Such differences might be expected due to the different hydrophobicity of the interiors of the hybrid and native PAMAM structures. In preliminary studies, we have established that the relative accessibility of the peripheral groups is similar as judged by synthetic transformation. In due course, studies where these hybrid structures are elaborated with additional layers of PAMAM chemistry will be communicated.

## Conclusion

Two high-purity triazine dendrimers that mimic the amphoteric surface of half-generation PAMAM dendrimers have been synthesized. Capillary electrophoresis and MALDI-TOF MS have been successfully employed in monitoring the progress of the reactions and determination of purity and dispersity. Capillary electrophoresis was also used to determine the pH range

within which fall the pI values of the respective dendrimers different between the two dendrimers. The triazine dendrimers, **2a** appears to be the preferred choice: the design exactly mirrors that of PAMAM dendrimers, synthesis proceeds with relative ease and final products are of significantly higher purity, approaching single entity systems. Although the synthesis of the dendrimer **1a** proceeds with more difficulty and results in a mixture of products, both capillary electrophoresis and MS confirm the dispersity to be much lower than that of commercially available PAMAM mixtures. Further, having pI values less than 7 provides sufficient aqueous solubility for all of the dendrimers under neutral and/or biological conditions. Overall, we believe the new hybrid triazine–PAMAM dendrimers could serve as alternatives to the widely studied and useful, but highly disperse commercially available PAMAM dendrimers.

**Acknowledgment.** This work was supported by the NIH (U01 5U01AI075351-02; R01 GM64560-07). We would like to thank the Laboratory for Molecular Simulation at Texas A&M University for providing software and computer resources.)

**Supporting Information Available:** Text discussing the selection of the BGE composition and preparation of BGE solutions, optimization of the MS analysis, and a detailed description of the 3-band PreMCE method and figures showing MS spectra, a plot of the band positions, and complete PreMCE traces recorded. This material is available free of charge via the Internet at <http://pubs.acs.org>.

## References and Notes

- (1) Eichman, J. D.; Bielinska, A. U.; Kukowska-Latallo, J. F.; Baker, J. R., Jr. *PSTT* **2000**, 3, 232–245.
- (2) (a) Lim, Y.; Kim, S.; Lee, Y.; Lee, W.; Yang, T.; Lee, M.; Suh, H.; Park, J. *J. Am. Chem. Soc.* **2001**, 123, 2460–2461. (b) Radu, D. R.; Lai, C.; Jeftinija, K.; Rowe, E. W.; Jeftinija, S.; Lin, V. S.-Y. *J. Am. Chem. Soc.* **2004**, 126, 13216–13217. (c) Choi, Y.; Baker, J. R., Jr. *Cell Cycle* **2005**, 4, 669–671.
- (3) (a) Dear, J. W.; Kobayashi, H.; Brechbiel, M. W.; Star, R. A. *Nephron. Clin. Pract.* **2006**, 103, c45–c49. (b) Xu, H.; Regino, C. A. S.; Koyama, Y.; Hama, Y.; Gunn, A. J.; Bernardo, M.; Kobayashi, H.; Choyke, P. L.; Brechbiel, M. W. *Bioconjugate Chem.* **2007**, 18, 1474–1482. (c) Waengler, C.; Waengler, B.; Eisenhut, M.; Haberkorn, U.; Mier, W. *Bioorg. Med. Chem.* **2008**, 16, 2606–2616.
- (4) (a) Wells, M.; Crooks, R. M. *J. Am. Chem. Soc.* **1996**, 118, 3988–3989. (b) Oh, E.; Hong, M.; Lee, D.; Nam, S.; Yoon, H. C.; Kim, H. *J. Am. Chem. Soc.* **2005**, 127, 3270–3271. (c) Mynar, J. L.; Lowery, T. J.; Wemmer, D. E.; Pines, A.; Frechet, J. M. J. *J. Am. Chem. Soc.* **2006**, 128, 6334–6335. (d) Das, J.; Aziz, Md. A.; Yang, H. *J. Am. Chem. Soc.* **2006**, 128, 16022–16023. (e) Ajikumar, P. K.; Ng, J. K.; Tang, Y. C.; Lee, J. Y.; Stephanopoulos, G.; Too, H. *Langmuir* **2007**, 23, 5670–5677.
- (5) (a) Watanabe, S.; Regen, S. L. *J. Am. Chem. Soc.* **1994**, 116, 8855–8856. (b) Miller, L. L.; Duan, R. G.; Tully, D. C.; Tomalia, D. A. *J. Am. Chem. Soc.* **1997**, 119, 1005–1010. (c) Yin, R.; Zhu, Y.; Tomalia, D. A.; Ibuki, H. *J. Am. Chem. Soc.* **1998**, 120, 2678–2679. (d) Kovvali, A. S.; Chen, H.; Sirkar, K. K. *J. Am. Chem. Soc.* **2000**, 122, 7594–7595. (e) Ispasoiu, R. G.; Balogh, L.; Varnavski, O. P.; Tomalia, D. A.; Goodson, T. III. *J. Am. Chem. Soc.* **2000**, 122, 11005–11006. (f) Gehringer, L.; Bourgogne, C.; Guillon, D.; Donnio, B. *J. Am. Chem. Soc.* **2004**, 126, 3856–3867.
- (6) (a) Chechik, V.; Zhao, M.; Crooks, R. M. *J. Am. Chem. Soc.* **1999**, 121, 4910–4911. (b) Niu, Y.; Yeung, L. K.; Crooks, R. M. *J. Am. Chem. Soc.* **2001**, 123, 6840–6846. (c) Liu, L.; Breslow, R. *J. Am. Chem. Soc.* **2003**, 125, 12110–12111. (d) Garcia-Martinez, J. C.; Lezutekong, R.; Crooks, R. M. *J. Am. Chem. Soc.* **2005**, 127, 5097–5103. (e) Jiang, Y.; Gao, Q. *J. Am. Chem. Soc.* **2006**, 128, 716–717.
- (7) Tomalia, D. A.; Baker, H.; Dewald, J.; Hall, M.; Kallos, G.; Martin, S.; Roeck, J.; Ryder, J.; Smith, P. *Polym. J.* **1985**, 17, 117–132.
- (8) Svenson, S.; Tomalia, D. A. *Adv. Drug Delivery Rev.* **2005**, 57, 2106–2129.
- (9) Myc, A.; Douce, T. B.; Ahuja, N.; Kotlyar, A.; Kukowska-Latallo, J.; Thomas, T. P.; Baker, J. R., Jr. *Anti-Cancer Drugs* **2008**, 19, 143–149.
- (10) Shi, X.; Majoros, I. J.; Baker, J. R., Jr. *Mol. Pharm.* **2005**, 2, 278–294.
- (11) (a) Caminade, A.-M.; Laurent, R.; Majoral, J.-P. *Adv. Drug Delivery Rev.* **2005**, 57, 2130–2146. (b) Shi, X.; Wojciech, L.; Islam, M. T.; Muniz, M. C.; Balogh, L. P.; Baker, J. R., Jr. *Colloids Surf., A* **2006**, 272, 139–150.
- (12) Chouai, A.; Simanek, E. E. *J. Org. Chem.* **2008**, 73, 2357–2366.
- (13) Lalwani, S.; Venditto, V. J.; Rivera, G. E.; Chouai, A.; Shaunak, S.; Simanek, E. E. *Macromolecules* **2009**, 42, 3152–3161.
- (14) Malik, N.; Wiwattanapatapee, R.; Klopsch, R.; Lorenz, K.; Frey, H.; Weener, J. W.; Meijer, E. W.; Paulus, W.; Duncan, R. *J. Controlled Release* **2000**, 65, 133–148.
- (15) El-Sayed, M.; Ginski, M.; Rhodes, C. A.; Ghandehari, H. *J. Bioact. Compat. Polym.* **2003**, 18, 7–22.
- (16) Shcharbin, D.; Drapeza, A.; Loban, V.; Lisichenok, A.; Bryszewska, M. *Cell. Mol. Biol. Lett.* **2006**, 11, 242–248.
- (17) Kaneta, T.; Ueda, T.; Hata, K.; Imasaka, T. *J. Chromatogr. A* **2006**, 1106, 52–55.
- (18) Williams, B. A.; Vigh, G. *Anal. Chem.* **1996**, 68, 1174–1180.
- (19) (a) Gas, B.; Coufal, P.; Jaros, M.; Muzikar, J.; Jelinek, I. *J. Chromatogr. A* **2001**, 905, 269–279. (b) Jaros, M.; Vcelakova, K.; Zuskova, K.; Gas, B. *Electrophoresis* **2002**, 23, 2667–2677. (c) Gas, B. <http://www.natur.cuni.cz/gas>.
- (20) Peterson, J.; Allikmaa, V.; Pehk, T.; Lopp, M. *Proc. Estonian Acad. Sci. Chem.* **2001**, 50, 167–172.
- (21) Glukhovskiy, P.; Vigh, G. *Electrophoresis* **1998**, 19, 3166–3170.
- (22) Nayak, N. C.; Shin, K. *Nanotechnology* **2008**, 19, 265603.
- (23) Martell, A. E.; Smith, R. M. *Critical Stability Constants, Volume 1: Amino Acids*; Plenum Press: New York, 1974; pp 1 and 20.
- (24) Hirt, R. C.; Schmitt, R. G. *Spectrochim. Acta* **1958**, 12, 127–138.